Molecular Cancer Therapeutics

Glucuronide-Linked Antibody–Tubulysin Conjugates Display Activity in MDR$^+$ and Heterogeneous Tumor Models

Patrick J. Burke, Joseph Z. Hamilton, Thomas A. Pires, Holden W.H. Lai, Christopher I. Leiske, Kim K. Emmerton, Andrew B. Waight, Peter D. Senter, Robert P. Lyon, and Scott C. Jeffrey

Abstract

Although antibody–drug conjugates (ADCs) find increasing applications in cancer treatment, *de novo* or treatment-emergent resistance mechanisms may impair clinical benefit. Two resistance mechanisms that emerge under prolonged exposure include upregulation of transporter proteins that confer multidrug resistance (MDR$^+$) and loss of cognate antigen expression. New technologies that circumvent these resistance mechanisms may serve to extend the utility of next-generation ADCs. Recently, we developed the quaternary ammonium linker system to expand the scope of conjugatable payloads to include tertiary amines and applied the linker to tubulysins, a highly potent class of tubulin binders that maintain activity in MDR$^+$ cell lines. In this work, tubulysin M, which contains an unstable acetate susceptible to enzymatic hydrolysis, and two stabilized tubulysin analogues were prepared as quaternary ammonium-linked glucuronide-linkers and assessed as ADC payloads in preclinical models. The conjugates were potent across a panel of cancer cell lines and active in tumor xenografts, including those displaying the MDR$^+$ phenotype. The ADCs also demonstrated potent bystander activity in a coculture model comprised of a mixture of antigen-positive and -negative cell lines, and in an antigen-heterogeneous tumor model. Thus, the glucuronide–tubulysin drug-linkers represent a promising ADC payload class, combining conjugate potency in the presence of the MDR$^+$ phenotype and robust activity in models of tumor heterogeneity in a structure-dependent manner. *Mol Cancer Ther; 17(8); 1752–60. ©2018 AACR.*

Introduction

In recent years, the tubulysins (1) have emerged as a compelling antimitotic payload class for drug-targeting applications, in part due to their high free drug potencies and retention of activity in multidrug resistant (MDR$^+$) cell lines (2). Mechanistically, they exert cytotoxic activity through disruption of microtubule dynamics resulting in collapse of the cytoskeleton, culminating in apoptotic cell death (3). Structurally, the tubulysins are tetrapeptides derived from *N*-methyl-D-pipecolic acid (Mep), L-isoleucine (Ile), tubuvaline (Tuv), and tubuphenylalanine (Tup) residues (Tup is substituted for tubutyrosine for the para-hydroxyphenyl-containing natural products). The most potent naturally occurring tubulysins, such as tubulysin D (**1**, Fig. 1), contain an N,O-acyl acetal functional group at the tertiary amide junction between the Ile and Tuv residues (4). Tubulysin D is reported to have EC_{50} values in the picomolar range in cytotoxicity assays (1, 5), whereas the corresponding secondary amide (tubulysin U, **2**) is less potent, with EC_{50} values typically in the nanomolar range (6, 7). However, in 2007, two groups demonstrated that replacement of the N,O-acyl acetal with a methyl group, creating N^{14}-desacetoxytubulysin H (hereafter referred to as tubulysin M, Tub(OAc), or **3**), resulted in minimal loss in potency (8, 9).

Although some evidence of activity was observed recently for a systemically administered tubulysin analogue (10), in many cases (11–13) tubulysins failed to provide a therapeutic window, and like other similar highly potent antimitotics (14, 15) may be too toxic for use as systemically administered chemotherapeutics. As a consequence, tubulysins continue to be investigated as payloads for a number of small molecule–(12, 16) and antibody–drug conjugates (17–22). For ADC applications, in which conjugates may be in circulation for many days to weeks, particular attention must be paid to the C11-acetoxy moiety in the Tuv residue, known to be an important structural element for high potency in both natural (23) and designed (19, 24) tubulysins. Loss of the acetate functional group results in >100-fold drop in potency and esterase-mediated deacetylation has been reported in plasma stability experiments (25). A cocrystal structure of Tub(OAc) bound to tubulin reveals that the C11-acetoxy resides at the solvent interface and a hydrophobic pocket and lacks direct contacts with the protein (26). To compensate for plasma deacetylation, we envisioned two strategies for stabilization of this moiety: replacement with a stable ethyl ether (**5**) and conversion to a branched ester (**6**), as increased steric

Seattle Genetics, Inc., Bothell, Washington.

Note: Supplementary data for this article are available at Molecular Cancer Therapeutics Online (http://mct.aacrjournals.org/).

Current address for H.W.H. Lai: Stanford University, Department of Chemistry, Palo Alto, California.

Corresponding Author: Patrick J. Burke, Seattle Genetics, Inc., 21823 30th Drive SE, Bothell, WA 98021. Phone: 425-527-4766; Fax: 425-527-4109; E-mail: pburke@seagen.com

doi: 10.1158/1535-7163.MCT-18-0073

hindrance of an ester functional group often leads to decreased esterase-mediated de-esterification (27–29).

The goal of this work was to evaluate the potential of tubulysin ADCs for activity in MDR$^+$ and antigen-heterogeneous tumor models and to investigate the impact of replacement of the tubuvaline acetate on conjugate activity. To achieve this, we applied the glucuronide quaternary ammonium linker system (30) to conjugate Tub(OAc) and the two stabilized analogues as ADC payloads for evaluation in preclinical experiments. The resulting conjugates displayed robust potency across a panel of cell lines and xenografts, including those displaying the MDR$^+$ phenotype. The ADCs also demonstrated bystander effects in both an *in vitro* coculture model and *in vivo* antigen-heterogeneous tumor model. These studies demonstrate that the tubulysins are an effective ADC payload to combine dual activity in MDR$^+$ and antigen-heterogeneous tumor models.

Materials and Methods

Preparation of ADCs bearing quaternary ammonium linkers

Tubulysin analogues **3** to **6** and glucuronide–tubulysin linkers **7** to **9** shown in Fig. 1 were synthesized as previously described (31–33). Antibody–drug conjugates loaded at 8 drugs/mAb (DAR 8) were prepared as follows. To achieve full reduction of the four native interchain disulfides, antibody in a PBS solution was bound to a MabSelectSuRe protein A column (GE Healthcare) and incubated with a large excess of tris(2-carboxyethyl)-phosphine (TCEP) for 30 minutes. The column was then washed thoroughly with PBS containing 5 mmol/L EDTA. The reduced mAb was eluted with 50 mmol/L glycine (pH 3.0), and the eluate was neutralized with an addition of concentrated sodium phosphate buffer to a final formulation of 80 mmol/L sodium phosphate, 50 mmol/L NaCl, 45 mmol/L glycine, 5 mmol/L EDTA, pH 7.4. Full reduction was confirmed by reversed-phase chromatography. Fully reduced antibody at approximately 10 mg/mL was conjugated with 10 molar equivalents (25% excess) of drug-linker as a 10 mmol/L DMSO stock. The resulting solution was vortexed and left at room temperature for 15 to 30 minutes. The extent of conjugation was assessed by reversed-phase chromatography, and additional drug-linker was added as needed. Once all available mAb cysteines were alkylated, excess drug-linker was removed via incubation with activated charcoal. The ADC was then buffer-exchanged into PBS using a NAP-5 desalting column (GE Healthcare). The extent of aggregation was assessed by size exclusion chromatography and in all cases monomeric ADCs were obtained. The final ADC concentration was measured spectrophotometrically, and the resulting ADCs (8-drugs/mAb) were sterile-filtered through a 0.22-μm centrifugal filter and stored at −80°C. For 4-loaded conjugates

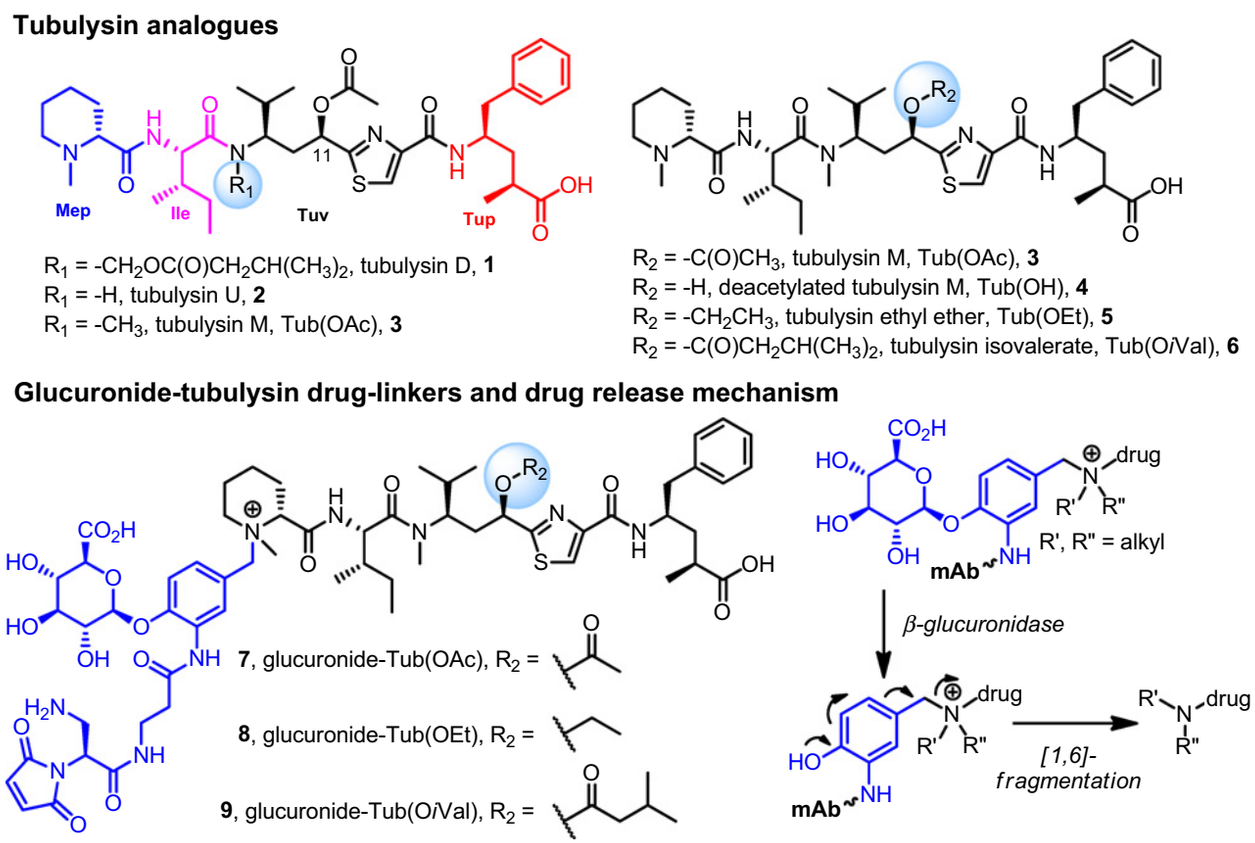

Figure 1.
Structures of tubulysin analogues and glucuronide–tubulysin drug-linkers.

(DAR 4), the reduction step was carried out in solution with substoichiometric TCEP to achieve partial reduction, revealing on average 4-thiols per mAb, and the subsequent conjugation, purification, and analysis were carried out as described above.

In vitro cytotoxicity assays

In vitro potency was assessed on multiple cancer cell lines: L540cy and L428 (Hodgkin lymphomas); Karpas299 (anaplastic large cell lymphoma (ALCL), originally provided by Dr. Abraham Karpas, University of Cambridge, Cambridge, UK), DEL, and DEL/BVR (ref. 34; anaplastic large cell lymphomas), HL60 and HL60/RV (acute myeloid leukemia lines), and U266luc (luciferase-transfected multiple myeloma) cell lines. The L540cy cell line was provided by Dr. Harald Stein (Institute fur Pathologie, University of Veinikum Benjamin Franklin, Berlin, Germany). The HL60/RV cell line was provided by Dr. David A. Scheinberg (Memorial Sloan Kettering Cancer Center, New York, NY). Karpas299, DEL, and L428 cell lines were obtained from DSMZ. The HL60 cell line and the U266 cells that were transfected with luciferase to provide U266luc (35) were obtained from ATCC. L540cy, L428, and Karpas299 cell lines were obtained in 2012. HL60 and U266 cell lines were obtained in 2013 and 2015, respectively. The cell lines were authenticated by STR profiling at IDEXX Bioresearch and cultured for no more than 2 months after resuscitation. Cells cultured in log-phase growth were seeded for 24 hours in 96-well plates containing 150 μL RPMI 1640 supplemented with 20% FBS. Serial dilutions of antibody–drug conjugates in cell culture media were prepared at 4× working concentrations, and 50 μL of each dilution was added to the 96-well plates. Following addition of test articles, cells were incubated with test articles for 4 days at 37°C. After 96 hours, growth inhibition was assessed by CellTiter-Glo (Promega), and luminescence was measured on a plate reader. The EC_{50} value, determined in triplicate, is defined here as the concentration that results in 50% reduction in cell growth relative to untreated controls.

Tubulin fluorescence polarization competition-binding assay

Sheep brain tubulin (SBT) was obtained from Cytoskeleton, and exact protein concentration was determined using the DC protein assay (Bio-Rad Laboratories). Eight point serial dilutions of test compounds were performed in assay buffer (20 mmol/L PIPES, pH 6.9, 1 mmol/L EGTA + 0.008% Tween 20) + 60 nmol/L FITC-MMAF probe for competition representing a 2× assay concentration (highest amount 250 μmol/L and dilutions occurring at 5× concentration). To initiate the assay, 15 μL of (2×) test compound dilution + 60 nmol/L FITC-MMAF was combined with 15 μl (2×) 600 nmol/L SBT in assay buffer in the wells of a 384-well plate for a final concentration of 30 nmol/L FITC-MMAF, 300 nmol/L SBT, and 8 test compound concentration points performed in triplicate. The plate was covered, and the binding competition was allowed to proceed for 1 hour at room temperature with gentle shaking. Fluorescence polarization was measured on an Envision multilabel reader (Perkin Elmer) using an installed FITC FP dual mirror. Measurements of polarization (milli-polarization units) are defined as (mP) = 1,000 $(S - G \times P)/(S + G \times P)$, where S and P represent the parallel and perpendicular background subtracted fluorescence count rates following polarized excitation, and G (grating) is an instrument-dependent factor calculated from pure fluorophore solution. Binding data were analyzed using GraphPad Prism software. EC_{50} values for the given assay conditions were calculated from a dose–response variable slope model given by the equation $[Y = \text{Bottom} + (\text{Top} - \text{Bottom})/(1 + 10^{((\text{LogEC50-X}) \times \text{HillSlope}))}]$. The binding affinities for each analogue are expressed as a ratio of the Tub(OAc) affinity, where RBA = Tub(OAc) EC_{50}/Tub analogue EC_{50}.

Mouse plasma stability experiments

Tubulysin ester stability was assessed in both free drug and conjugate form. Tubulysin analogues Tub(OAc), Tub(OEt), and Tub(O*i*Val) were incubated in mouse plasma or cell culture media containing 20% fetal bovine serum at 37°C for 5 days. At multiple time points (0, 1, 4, 8, 24, 48, and 120 hours) samples were taken and diluted in ice-cold methanol. The protein precipitates were removed by centrifugation at 12,000 × *g* for 10 minutes. The supernatant was collected and analyzed by reversed phase UPLC (Waters Acquity H Class Alliance) with mass spectrometric detection (Waters Xevo G2 TOF), counting ions for intact drug and de-esterified Tub(OH). Tubulysin ester stability in conjugate form was assessed by incubating DAR 8 anti-CD30 tubulysin ADCs in mouse plasma and analyzing ester integrity of the conjugated drug over time. After 3 and 7 days of incubation at 37°C, plasma aliquots were purified using anti-human capture affinity resin (IgSelect, GE Healthcare) for two hours at 2 to 8°C. The bound samples were washed using 0.5 mol/L NaCl and eluted using 50 mmol/L glycine, pH 3. Eluted samples were deglycosylated using PNGase F (New England BioLabs Inc.) and then reduced using 5 mmol/L DTT. Each sample was analyzed using reversed-phased UPLC (PLRP xum, Agilent) coupled with mass spectrometric detection (Waters Xevo G2-S QTOF). Intact tubulysin ester (% ester intact) was calculated using total ion counts of the drug-loaded light chain and heavy chain species, assessed by a loss of 42 and 84 Daltons for Tub(OAc) and Tub(O*i*Val), respectively.

In vivo xenograft models

All experiments were conducted in concordance with the Institutional Animal Care and Use Committee in a facility fully accredited by the Association for the Assessment and Accreditation of Laboratory Animal Care. Therapy experiments were conducted in three xenograft models: L540cy ($CD30^+/MDR^-$ Hodgkin lymphoma), DEL/BVR ($CD30^+/MDR^+$ anaplastic large cell lymphoma), and Karpas/KarpasBVR ($CD30^+/CD30^-/MDR^-$ anaplastic large cell lymphoma), an antigen-heterogeneous model of bystander activity. Tumor cells, as a suspension, were implanted subcutaneously in immunocompromised SCID mice. For the Karpas/KarpasBVR bystander activity tumor model, implantation was performed with a 1:1 admixture of $CD30^+$ Karpas299 and $CD30^-$ KarpasBVR cells. Upon tumor engraftment, mice were randomized to study groups once the average tumor volume reached approximately 100 mm^3. For all *in vivo* experiments, ADCs were conjugated at 4-drugs/Ab as higher DAR 8 loading of drug-linker **7** has been previously shown to decrease ADC exposure (30). The ADCs were dosed once by intraperitoneal injection. Tumor volume as a function of time was determined using the formula $(L \times W^2)/2$. Animals were euthanized when tumor volumes reached 1,000 mm^3.

Results

Drug-linker design

Early work on tubulysin natural products demonstrates the importance of the C11-acetoxy group for high cellular potency (23). Given the propensity of esters to hydrolyze *in vivo*, commonly due to esterase activity, we generated tubulysin analogues with stabilized moieties at the C11 position. Given that the tubulysin M-tubulin cocrystal structure (26) indicates that the acetoxy group lacks direct contacts and resides at the interface between a hydrophobic pocket and solvent, we surmised that conversion of the acetate to either a more sterically hindered ester or an ether should be tolerated for tubulin binding. To test this, we prepared and evaluated a panel of tubulysin ether and ester analogues, with tubulysin ethyl ether (Tub(OEt), **5**) and tubulysin isovalerate (Tub(O*i*Val), **6**) emerging as leads (31). In the work presented here, we evaluated Tub(OAc) and the stabilized analogues, Tub(OEt) and Tub(O*i*Val), as ADC payloads with emphasis on their activities in MDR^+ and antigen-heterogeneous models.

The tubulysin analogues were conjugated at their N-terminal tertiary amine groups providing glucuronide quaternary ammonium drug-linkers **7** to **9**. The glucuronide linker system (32) is a hydrophilic, cleavable linker that exploits intracellular β-glucuronidase to facilitate drug release. The quaternary ammonium drug-linkers were prepared through alkylation of a benzyl bromide intermediate with the tertiary amine residue in the tubulysin analogues, as described in the Supplementary Information. A self-stabilizing maleimide (mDPR) was incorporated as the point of attachment between the drug-linkers and antibody cysteine residues for enhanced *in vivo* stability (36).

Tubulysin free drug potency and ester stability

Prior to evaluation as ADC payloads, tubulysins **3** to **6** were screened as free drugs *in vitro* for cellular and biochemical potency, as shown in Table 1. The analogues were evaluated on a panel of lymphoma and leukemia cell lines, including MDR^+ L428 and HL60/RV cells. Consistent with previous reports (19, 23, 24), the deacetylated tubulysin analogue Tub(OH) was 70- to 1,000-fold less potent than the parental drug. In contrast, the two stabilized analogues, Tub(OEt) and Tub(O*i*Val), displayed levels of cytotoxic potency similar to Tub(OAc) on L540cy, L428, and HL60 cell lines. On MDR^+ HL60/RV cells, Tub(OAc) was approximately 6-fold more potent than Tub(OEt) and Tub(O*i*Val). Biochemical potency was assessed using a competitive fluorescence polarization tubulin binding assay. Consistent with the cell potency results, deacetylated analogue Tub(OH) was noncompetitive in the tubulin binding assay, highlighting the importance of an ether or ester group at the C11 position. The stabilized analogues Tub(OEt) and Tub(O*i*Val) displayed tubulin affinities of 0.89 and 0.26, respectively, relative to Tub(OAc), indicating a partial diminution of tubulin affinity.

To confirm that the branched ester functional group in Tub(O*i*Val) would enhance stability relative to the acetate in Tub(OAc), multiple stability experiments were performed. Free drugs Tub(OAc), Tub(OEt), and Tub(O*i*Val) were incubated for 5 days in cell culture media and mouse plasma at 37°C and monitored for integrity at various time points. The ether moiety in Tub(OEt) was found to be completely stable in mouse plasma (Fig. 2A) and cell culture media (Supplementary Fig. S1). The branched ester group in Tub(O*i*Val) confers significantly increased stability relative to the acetate in Tub(OAc). At 48 hours, Tub(O*i*Val) was 92% and 91% intact in cell culture media and mouse plasma, respectively, compared with 46% and 54% acetate intact for Tub(OAc) (Table 1). We also assessed ester stability as conjugated payloads, knowing that antibody conjugation can affect the stability of hydrolytically labile functional groups (37). DAR 8 αCD30 ADCs bearing the gluc-Tub(OAc) drug-linker **7** or gluc-Tub(O*i*Val) drug-linker **9** were incubated in mouse plasma at 37°C. Samples were analyzed at 3 and 7 days of incubation for ester integrity by mass spectrometry. As shown in Fig. 2B, increased ester stability was observed for the conjugate bearing Tub(O*i*Val), with 94% ester intact at 7 days. At the same time point, the ester was 68% intact for the Tub(OAc) conjugate. Thus, steric hindrance in the ester side-chain appears to increase stability in cell culture media and plasma in free drug and conjugated form. Finally, gluc-Tub(OAc) drug-linker **7** was assessed for stability *in vivo*. Mice were dosed at 3 mg/kg with conjugate bearing drug-linker **7**, and ADC was analyzed for drug integrity at 4 and 10 days after dose. The acetate in gluc-Tub(OAc) was found to be 83% and 70% intact at 4 and 10 days after dose, respectively (Supplementary Fig. S2).

Tubulysin ADCs *in vitro* cytotoxicity

Anti-CD30 DAR 8 conjugates loaded with drug-linkers **7** to **9** bearing potent tubulysins Tub(OAc), Tub(OEt), and Tub(O*i*Val), respectively, were evaluated on a panel of $CD30^+$ lymphoma cell lines, including two MDR^+ strains, and in an antigen-heterogeneous *in vitro* model of bystander activity. In the $CD30^+$, MDR^- cell lines L540cy, Karpas299, and DEL, all three tubulysin ADCs displayed potent cytotoxic activity with EC_{50}s in the single-digit ng/mL range, as shown in Table 2. The

Table 1. Free drug *in vitro* properties

Cytotoxicity[a], relative tubulin binding affinity, and stability								
							% Intact at 48 hours, 37°C	
Compound	Drug	L540cy, HL	L428[b], HL	HL60, AML	HL60/RV[b], AML	Tubulin RBA[c]	Cell media	Mouse plasma
3	Tub(OAc)	0.14 nmol/L	0.039	0.15	1.0	1.0	46%	54%
4	Tub(OH)	19	62	11	>1,000	NC[d]	NA	NA
5	Tub(OEt)	0.086	0.13	0.093	5.8	0.89	100%	100%
6	Tub(O*i*Val)	0.062	0.11	0.045	5.8	0.26	92%	91%

[a]Following 96 hours treatment, cells were assessed for viability as described in the Materials and Methods.
[b]MDR-positive by rhodamine efflux.
[c]Biochemical potency: tubulin RBA = ratio of Tub(OAc) EC_{50}/Tub analogue EC_{50}.
[d]NC, noncompetitive.

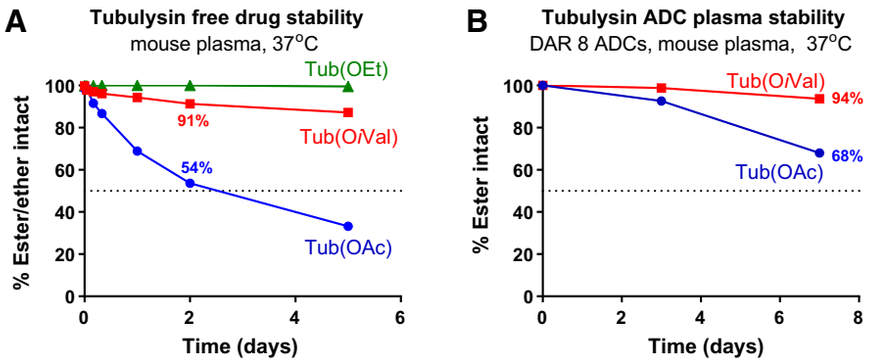

Figure 2.

Tubuvaline ester stability in mouse plasma at 37°C for (**A**) free drugs and (**B**) antibody–drug conjugates. **A,** Tubulysin free drugs were incubated in plasma and assessed by LC/MS for structural integrity. The ether and hindered ester analogues displayed increased stability relative to Tub(OAc). **B,** Anti-CD30 antibodies were conjugated at 8 drugs/Ab with drug-linkers **7** and **9**. ADCs were incubated in mouse plasma and analyzed for ester integrity at 3- and 7-day time points. The branched isovalerate ester at the tubuvaline residue in drug-linker **9** displayed improved stability relative to the acetate in drug-linker **7**.

ADC activities were immunologically specific, with EC_{50} > 1,000 ng/mL (the highest concentration tested) against the $CD30^-$ U266luc cell line. In contrast, structure-dependent activity was observed in the $CD30^+$, MDR^+ DEL/BVR, and L428 lymphoma cell lines. In this case, the Tub(OAc) conjugate had the highest level of potency with EC_{50}s of 3.3 and 0.46 ng/mL on DEL/BVR and L428, respectively. The ADC bearing stabilized analogue Tub(OEt) was comparable with the Tub(OAc) conjugate on DEL/BVR, but 10-fold less potent on L428 cells. Finally, the αCD30 ADC containing Tub(O*i*Val) stabilized analogue as the payload was less potent than the Tub(OAc) counterpart on both MDR^+ cell lines, with >100-fold attenuation in activity observed.

The αCD30 tubulysin ADCs were further evaluated in a heterogeneous $CD30^+/CD30^-$ coculture model of bystander activity, in which a 1:1 mixture of $CD30^+$ L540cy and $CD30^-$ U266luc cells were treated with the conjugates. ADC payloads endowed with bystander activity are capable of killing both cell populations via diffusion of drug released in antigen-positive cells (L540cy, in this case) to neighboring antigen-negative (U266luc) cells (35). Dose–response curves for the tubulysin ADCs are shown in Fig. 3. The CD30-targeted ADCs (shown in closed symbols) composed of Tub(OAc), Tub(OEt), and Tub(O*i*Val) potently inhibited the growth of both cell populations, with the stabilized analogues providing a 2- to 3-fold shift toward greater potency relative to Tub(OAc). The non-binding control ADCs, shown as open symbols, were inactive.

In vivo xenograft and tolerability experiments

The tubulysin ADCs were evaluated in three different xenograft models: a $CD30^+$, MDR^- L540cy Hodgkin lymphoma model; a $CD30^+$, MDR^+ DEL/BVR ALCL xenograft; and in the MDR^-, $CD30^+/CD30^-$ Karpas/KarpasBVR admixed xenograft bystander activity model (38). Previous work established that DAR 8 loading of drug-linker **7** resulted in decreased ADC exposure (30); thus, the αCD30 ADCs were conjugated at 4 drugs/Ab with glucuronide–tubulysin linkers **7** to **9**. Mice bearing L540cy xenografts were administered a single i.p. dose once the average tumor volume reached 100 mm^3. Mean tumor volume as a function of time is shown in Fig. 4A and B, and complete regressions and cures are tabulated in Table 3. Following a single dose of 0.15 or 0.3 mg/kg, the Tub(OAc) conjugate (αCD30-**7**) displayed a similar extent of averaged tumor growth delay compared with Tub(OEt)-based αCD30-**8** (Fig. 4A). At the higher dose of 0.3 mg/kg 1 of 6 and 2 of 6 mice were cured for the Tub(OAc) and Tub(OEt) groups, respectively (Table 3). Stabilized analogue Tub(O*i*Val) was compared with Tub(OAc) at higher doses of 0.25 and 0.5 mg/kg, shown in Fig. 4B. Here again, a similar level of antitumor activity was observed for the αCD30-**7** Tub(OAc) conjugate relative to the αCD30-**9** Tub(O*i*Val) comparator, with similar numbers of

Table 2. EC_{50} values[a] (ng ADC/mL) for αCD30 glucuronide-based DAR 8 ADCs

ADC cytotoxicity					
CD30 expression, MDR status	**Cell line**	**ADC: payload:**	**αCD30-7 Tub(OAc)**	**αCD30-8 Tub(OEt)**	**αCD30-9 Tub(O*i*Val)**
$CD30^+$, MDR^-	L540cy, HL		1.1 ng/mL	4.6	2.1
	Karpas299, ALCL		0.65	0.93	0.90
	DEL, ALCL		2.1	1.8	0.90
$CD30^+$, MDR^+	DEL/BVR, ALCL		3.3	4.7	390 (48%)[b]
	L428, HL		0.46 (17%)	4.3 (29%)	>1,000 (58%)
$CD30^-$, MDR^-	U266luc, MM		>1,000	>1,000	>1,000
1:1 $CD30^+$:$CD30^-$, MDR^-	1:1 L540cy:U266luc		5.6	2.4	1.8

[a]Cells were treated for 96 hours, then assessed for cell viability as described in Materials and Methods.
[b]%Viability is shown when >10% at the highest dose tested.

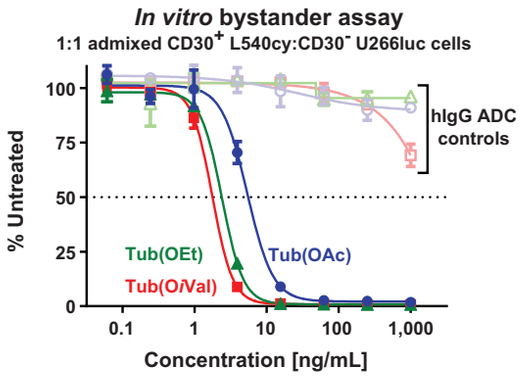

Figure 3.

In vitro activity of αCD30 DAR 8 ADCs bearing glucuronide-tubulysin drug-linkers containing the acetate (**7**), ethyl ether (**8**), and isovalerate (**9**) functional groups in a model of bystander activity. A 1:1 mixture of $CD30^+$ L540cy and $CD30^-$ U266luc cells were treated with ADCs for 96 hours, and then cellular growth inhibition was assessed as described. All three tubulysin ADCs displayed immunological specificity, with increased potency observed for conjugates bearing the drug-linkers (**8** and **9**) containing stabilized analogues.

mice cured at both doses (Table 3). In conclusion, in the MDR^- model, all three αCD30 tubulysin ADCs displayed similar potencies.

The tubulysin conjugates were then evaluated in MDR^+ and antigen-heterogeneity resistance models. SCID mice xenografted with $CD30^+$, MDR^+ DEL/BVR anaplastic large cell lymphoma tumors were administered a single i.p. dose when tumor volumes reached 100 mm^3, as shown in Fig. 4C. The Tub(OAc) αCD30-7 conjugate was curative in 5 of 5 animals when dosed at 1 mg/kg. The stabilized analogues were less potent at equivalent or similar doses, with 1 of 5 and 1 of 6 mice cured (Table 3) in groups treated with ADCs bearing Tub(OEt) and Tub(O*i*Val), respectively. Bystander activity in a heterogeneous tumor model was assessed in the Karpas/KarpasBVR admixed tumor xenograft. In this MDR-negative model, tumors are composed of a 1:1 mixture of $CD30^+$ Karpas299 cells and $CD30^-$ KarpasBVR cells, which evolved resistance to continuous brentuximab vedotin exposure through downregulation of CD30 (38). Mice bearing heterogeneous tumors were treated once i.p. with αCD30 tubulysin conjugates, tumor volume as a function of time for each animal is plotted in Fig. 4D following the 0.5 mg/kg dose. In all three treatment groups, most of the animals experienced complete regressions; however, the effects appeared to be more durable for those treated with ADCs composed of the stabilized tubulysins (Table 3).

To approximate the therapeutic window of the tubulysin ADCs, humanized IgG DAR 4 conjugates bearing Tub(OAc) drug-linker **7** or Tub(OEt) drug-linker **8** were evaluated for tolerability in Sprague–Dawley rats. Stabilized payload Tub(OEt) was prioritized over Tub(O*i*Val) due to the improved activity of the former in the MDR^+ cell lines (Table 2). As described in the Supplementary Information, rats ($n = 3$) were administered a single 10 mg/kg i.v. dose of conjugate and monitored for clinical observations and weight loss as a function of time. Over the course of the 28-day experiment, weight loss (Supplementary Fig. S3) or outward signs of toxicity were not observed. Thus, the tubulysin ADCs were highly potent in the xenograft models at well-tolerated dose levels.

Discussion

As ADCs (39) find increased clinical application, *de novo* or treatment-related resistance mechanisms could limit patient benefit and new technologies that circumvent these factors may be important design considerations for next-generation ADCs. Two resistance mechanisms that emerge under prolonged exposure to monomethylauristatin E (MMAE)-based ADCs like brentuximab vedotin and pinatuzumab vedotin include upregulation of ATP-binding cassette (ABC) efflux pumps that confer the MDR^+ phenotype and downregulation of CD30 expression (34, 38, 40, 41). These findings, coupled with the observation that some solid tumors are MDR^+ and/or display antigen heterogeneity initially (42–44), inspired us to evaluate alternative antimitotic payloads capable of regressing MDR^+ tumors and exerting bystander effects.

The tubulysins are a compelling class of cytotoxics, in part due to their high free drug potencies and retention of activity in MDR^+ cell lines, properties required to overcome the aforementioned resistance mechanisms. For use in antibody–drug conjugates, careful attention must be paid to the hydrolytically unstable ester groups present in many of the most potent natural products, as antibodies (and ADCs) are known to remain in circulation for many days. Early SAR work established the N,O-acyl acetal at the Ile-Tuv tertiary amide junction as nonessential for high potency (8, 9). However, replacement of the C11-acetoxy group with complete retention of potency has proven more difficult. Several acetate isosteres, including amides (45), carbamates (19, 25, 46), and ethers (7, 45–47), have been tried with mixed results. Conversion of the tubulysin acetate to the corresponding acetamide resulted in decreased free drug potency (45). Cong and coworkers replaced the TubM acetate with an *N*-methyl carbamate and observed a 5-fold reduction in drug potency (46). More recently, Tumey and coworkers reported on the substitution of the acetate in a tubulysin analogue to an *N*-ethyl carbamate for ADC applications, observing comparable *in vitro* free drug potency and enhanced plasma stability (25). However, while the resulting ADCs proved potent and selective, the authors noted that this approach did not offer an improvement in activity *in vivo*.

Tubulysin analogues in which the acetate has been replaced with an ether moiety are known (7, 45, 46). Recently, Staben and coworkers reported on the replacement of the TubM acetate with an ether to overcome *in vivo* deacetylation of MC-ValCit-TubM ADCs (22). In this case, the *N*-methyl group at the Ile-Tuv tertiary amide junction was replaced with an *N*-propyl group, and the C11 acetate was substituted with a propyl ether. Anti-CD22 ADCs containing the tubulysin propyl ether were found to be slightly less potent than the MMAE comparator in the MDR-negative lymphoma model. Whereas in the MDR^+ lymphoma tumor model the tubulysin propyl ether ADC induced transient tumor growth delay at the highest dose tested and the activity exceeded that of the comparator bearing MMAE, a payload known to possess bystander effects (38) but attenuated activity in MDR^+ models (35, 41, 48). The propyl ether was posited as a stabilized improvement over TubM, enabling activity in multidrug-resistant tumors. However, TubM was not included in the MDR^+ xenograft,

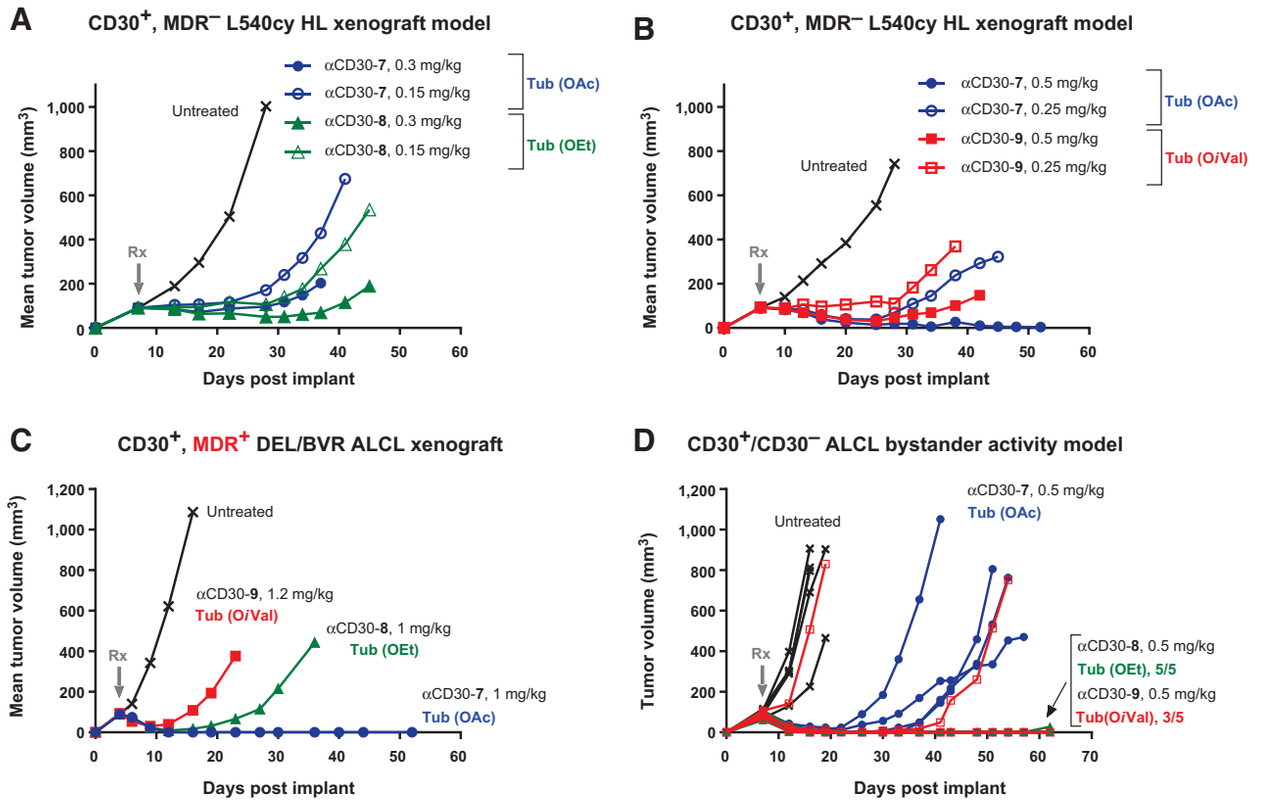

Figure 4.
Antitumor activities of anti-CD30 conjugates bearing glucuronide–tubulysin linkers loaded at 4 drugs/Ab. In each experiment, mice were administered a single intraperitoneal dose once average tumor volume reached 100 mm^3. Plotting was discontinued once tumor volume exceeded 1,000 mm^3 for at least one animal in **A–C**. **A** and **B,** Mice bearing $CD30^+$, MDR^- L540cy Hodgkin lymphoma xenografts were treated with conjugates containing the tubulysin acetate (drug-linker **7**) and ethyl ether (drug-linker **8**) in **A**, whereas tubulysin acetate (drug-linker **7**) and tubulysin isovalerate (drug-linker **9**) were compared in **B**. All three conjugates displayed similar potency in the MDR^- Hodgkin lymphoma model. **C,** Mice bearing $CD30^+$, MDR^+ DEL/BVR anaplastic large cell lymphoma xenografts were cured (5 of 5 animals) following treatment with conjugate bearing the tubulysin acetate (drug-linker **7**), whereas the stabilized analogues provided tumor growth delay. **D,** All three conjugates bearing tubulysin linkers displayed activity in the $CD30^+/CD30^-$ admixed tumor model of bystander activity, with a greater fraction of mice cured (see Table 3) following treatment with the stabilized tubulysin analogues.

making it unclear if the stabilized analogue offers an improvement in activity in the resistant *in vivo* model.

In contrast, we found MDR^+ models to be more sensitive to Tub(OAc) (or TubM) ADC relative to those composed of stabilized analogues, Tub(OEt) and Tub(O*i*Val). As free drugs, Tub(OAc) was marginally more potent than the stabilized analogues Tub(OEt) and Tub(O*i*Val) on the MDR^+ cancer cell lines (Table 1). As anti-CD30 ADCs, the differences were more pronounced. While similar in MDR^+ DEL/BVR, Tub(OEt)-based ADC αCD30-**8** was ∼10-fold less potent on MDR^+ L428 cells than the Tub(OAc) comparator (Table 2). The stabilized ester Tub(O*i*Val)-based conjugate, αCD30-**9**, was attenuated in both MDR^+ cells lines, with EC_{50}s > 100-fold less potent than the Tub(OAc) version (Table 2). *In vivo*,

Table 3. Summary of *in vivo* activity for αCD30 glucuronide–tubulysin DAR 4 ADCs

		ADC: payload:	αCD30-7 Tub(OAc)		αCD30-8 Tub(OEt)		αCD30-9 Tub(O*i*Val)	
Xenograft	Dose (mg/kg)	n/group	CR[a]	Cures	CR	Cures	CR	Cures
$CD30^+$, MDR^- L540cy HL	0.15	6	0	0	1	0		
	0.3	6	1	1	2	2		
	0.25	6	1	1			1	1
	0.5	6	6	4			4	3
$CD30^+$, MDR^+ DEL/BVR ALCL	1	5	5	5	2	1		
	1.2	6					1	1
1:1 $CD30^+$:$CD30^-$ Karpas/KarpasBVR bystander model	0.5	5	3	1	5	4	4	3
	1.5	5	3	0	4	3	5	4

[a]Complete regression observed following ADC treatment and includes durable and transient complete regressions.

Tub(OAc)-containing αCD30-7 was more active than the stabilized conjugates in the MDR$^+$ DEL/BVR xenograft (Fig. 4C). The origins of these differences are unclear at this time but may be due to differences in tubulin binding affinities and susceptibility to efflux transporters.

While the Tub(OAc) conjugate was more potent in MDR$^+$ experiments, the bystander activity models were more sensitive to αCD30 ADCs bearing stabilized tubulysins. In an *in vitro* coculture model, conjugates bearing stabilized analogues Tub(OEt) and Tub(O*i*Val) were equipotent, while the Tub(OAc) ADC was 2- to 3-fold less potent (Table 2; Fig. 3). This trend translated *in vivo*. In the ALCL bystander activity model (Fig. 4D) composed of CD30$^+$ and CD30$^-$ tumor cells, a single dose of 0.5 mg/kg of αCD30 ADCs bearing either Tub(OEt) or Tub(O*i*Val) resulted in cures in most of the mice, whereas the Tub(OAc) conjugate provided transient regressions with 1 of 5 mice cured (Table 3). We hypothesize that these activity trends may be due to Tub(OAc) deacetylation and physicochemical differences between the tubulysin analogues. To exert a bystander effect, the tubulysin payload must internalize into a CD30$^+$ cell, traffic to lysosomes for payload release, diffuse out of the CD30$^+$ cell into the cell culture media (*in vitro*) or extracellular matrix (*in vivo*), and then diffuse into a proximal CD30$^-$ cell to achieve a cell kill in the untargeted, antigen-negative population. Cumulative loss of the acetate from the CD30-delivered Tub(OAc) relative to the stabilized analogues may contribute to the decrease in potency. By way of illustration, the ester group in Tub(OAc) was 54% hydrolyzed over 48 hours in cell culture media (Table 1) compared with 8% for Tub(O*i*Val) under the same conditions. Physicochemical properties may also be playing a role, as increased analogue hydrophobicity would facilitate diffusion across plasma membranes. For example, the hydrophobicity as estimated by cLogP for Tub(OEt) and Tub(OAc) is 2.9 and 2.4, respectively, perhaps endowing greater diffusivity for the stabilized analogue.

Based on the composite activity data, the Tub(OAc) and Tub(OEt) linkers emerged as the leads and were assessed for rat tolerability. A single i.v. dose at 10 mg/kg of αCD30-7 or αCD30-8 was well tolerated, providing evidence of >10-fold therapeutic window in rodents for these new technologies. A more detailed toxicological evaluation would be warranted in the context of an ADC progressing toward clinical trials. Selection of a preferred tubulysin linker in that scenario would likely be a function of antigen target characteristics and indication-specific tumor biology. The tubulysin payload leads described here displayed activity in preclinical models of multidrug resistance and antigen heterogeneity and are the subject of ongoing investigation for future ADC programs.

Disclosure of Potential Conflicts of Interest

No potential conflicts of interest were disclosed.

Authors' Contributions

Conception and design: P.J. Burke, J.Z. Hamilton, P.D. Senter, R.P. Lyon, S.C. Jeffrey

Development of methodology: J.Z. Hamilton, H.W.H. Lai

Acquisition of data (provided animals, acquired and managed patients, provided facilities, etc.): J.Z. Hamilton, T.A. Pires, H.W.H. Lai, C.I. Leiske, K.K. Emmerton, A.B. Waight

Analysis and interpretation of data (e.g., statistical analysis, biostatistics, computational analysis): P.J. Burke, J.Z. Hamilton, P.D. Senter

Writing, review, and/or revision of the manuscript: P.J. Burke, J.Z. Hamilton, T.A. Pires, P.D. Senter, S.C. Jeffrey

Study supervision: P.J. Burke, K.K. Emmerton, P.D. Senter

The costs of publication of this article were defrayed in part by the payment of page charges. This article must therefore be hereby marked *advertisement* in accordance with 18 U.S.C. Section 1734 solely to indicate this fact.

Received January 19, 2018; revised March 6, 2018; accepted May 18, 2018; published first June 4, 2018.

References

1. Sasse F, Steinmetz H, Heil J, Hofle G, Reichenbach H. Tubulysins, new cytostatic peptides from myxobacteria acting on microtubuli. Production, isolation, physico-chemical and biological properties. J Antibiot 2000;53:879–85.
2. Kaur G, Hollingshead M, Holbeck S, Schauer-Vukasinovic V, Camalier RF, Domling A, et al. Biological evaluation of tubulysin A: a potential anticancer and antiangiogenic natural product. Biochem J 2006;396: 235–42.
3. Khalil MW, Sasse F, Lunsdorf H, Elnakady YA, Reichenbach H. Mechanism of action of tubulysin, an antimitotic peptide from myxobacteria. ChemBioChem 2006;7:678–83.
4. Chai Y, Pistorius D, Ullrich A, Weissman KJ, Kazmaier U, Muller R. Discovery of 23 natural tubulysins from Angiococcus disciformis An d48 and Cystobacter SBCb004. Chem Biol 2010;17:296–309.
5. Ullrich A, Chai Y, Pistorius D, Elnakady YA, Herrmann JE, Weissman KJ, et al. Pretubulysin, a potent and chemically accessible tubulysin precursor from Angiococcus disciformis. Angew Chem Int Ed Engl 2009; 48:4422–5.
6. Shankar SP, Bigotti F, Lazzari P, Manca I, Spiga M, Sani M, et al. Synthesis and cytotoxicity evaluation of diastereomers and N-terminal analogues of tubulysin-U. Tet Lett 2013;54:6137–41.
7. Shankar SP, Jagodzinska M, Malpezzi L, Lazzari P, Manca I, Greig IR, et al. Synthesis and structure-activity relationship studies of novel tubulysin U analogues–effect on cytotoxicity of structural variations in the tubuvaline fragment. Org Biomol Chem 2013;11:2273–87.
8. Patterson AW, Peltier HM, Sasse F, Ellman JA. Design, synthesis, and biological properties of highly potent tubulysin D analogues. Chemistry 2007;13:9534–41.
9. Wang Z, McPherson PA, Raccor BS, Balachandran R, Zhu G, Day BW, et al. Structure-activity and high-content imaging analyses of novel tubulysins. Chem Biol Drug Des 2007;70:75–86.
10. Sani M, Lazzari P, Folini M, Spiga M, Zuco V, De Cesare M, et al. Synthesis and superpotent anticancer activity of tubulysins carrying non-hydrolysable N-substituents on tubuvaline. Chem Eur J 2017;23:5842–50.
11. Floyd WC 3rd, Datta GK, Imamura S, Kieler-Ferguson HM, Jerger K, Patterson AW, et al. Chemotherapeutic evaluation of a synthetic tubulysin analogue-dendrimer conjugate in c26 tumor bearing mice. ChemMedChem 2011;6:49–53.
12. Leamon CP, Reddy JA, Vetzel M, Dorton R, Westrick E, Parker N, et al. Folate targeting enables durable and specific antitumor responses from a therapeutically null tubulysin B analogue. Cancer Res 2008;68:9839–44.
13. Schluep T, Gunawan P, Ma L, Jensen GS, Duringer J, Hinton S, et al. Polymeric tubulysin-peptide nanoparticles with potent antitumor activity. Clin Cancer Res 2009;15:181–9.
14. Perez EA, Hillman DW, Fishkin PA, Krook JE, Tan WW, Kuriakose PA, et al. Phase II trial of dolastatin-10 in patients with advanced breast cancer. Invest New Drugs 2005;23:257–61.
15. von Mehren M, Balcerzak SP, Kraft AS, Edmonson JH, Okuno SH, Davey M, et al. Phase II trial of dolastatin-10, a novel anti-tubulin agent, in metastatic soft tissue sarcomas. Sarcoma 2004;8:107–11.

16. Reddy JA, Dorton R, Dawson A, Vetzel M, Parker N, Nicoson JS, et al. In vivo structural activity and optimization studies of folate-tubulysin conjugates. Mol Pharm 2009;6:1518–25.
17. Cohen R, Vugts DJ, Visser GW, Stigter-van Walsum M, Bolijn M, Spiga M, et al. Development of novel ADCs: conjugation of tubulysin analogues to trastuzumab monitored by dual radiolabeling. Cancer Res 2014;74:5700–10.
18. Harper J, Lloyd C, Dimasi N, Toader D, Marwood R, Lewis L, et al. Preclinical evaluation of MEDI0641, a pyrrolobenzodiazepine-conjugated antibody-drug conjugate targeting 5T4. Mol Cancer Ther 2017;16:1576–87.
19. Leverett CA, Sukuru SCK, Vetelino BC, Musto S, Parris K, Pandit J, et al. Design, synthesis, and cytotoxic evaluation of novel tubulysin analogues as ADC payloads. ACS Med Chem Lett 2016;7:999–1004.
20. Li JY, Perry SR, Muniz-Medina V, Wang X, Wetzel LK, Rebelatto MC, et al. A biparatopic HER2-targeting antibody-drug conjugate induces tumor regression in primary models refractory to or ineligible for HER2-targeted therapy. Cancer Cell 2016;29:117–29.
21. Nicolaou KC, Erande RD, Yin J, Vourloumis D, Aujay M, Sandoval J, et al. Improved total synthesis of tubulysins and design, synthesis, and biological evaluation of new tubulysins with highly potent cytotoxicities against cancer cells as potential payloads for antibody-drug conjugates. J Amer Chem Soc 2018;140:3690–711.
22. Staben LR, Yu S, Chen J, Yan G, Xu Z, Rosario GD, et al. Stabilizing a tubulysin antibody-drug conjugate to enable activity against multidrug-resistant tumors. ACS Med Chem Lett 2017;8:1037–41.
23. Balasubramanian R, Raghavan B, Begaye A, Sackett DL, Fecik RA. Total synthesis and biological evaluation of tubulysin U, tubulysin V, and their analogues. J Med Chem 2009;52:238–40.
24. Toader D, Wang F, Gingipalli L, Vasbinder M, Roth M, Mao S, et al. Structure-cytotoxicity relationships of analogues of N14-desacetoxytubulysin H. J Med Chem 2016;59:10781–7.
25. Tumey LN, Leverett CA, Vetelino B, Li F, Rago B, Han X, et al. Optimization of tubulysin antibody-drug conjugates: a case study in addressing ADC metabolism. ACS Med Chem Lett 2016;7:977–82.
26. Wang Y, Benz FW, Wu Y, Wang Q, Chen Y, Chen X, et al. Structural insights into the pharmacophore of vinca domain inhibitors of microtubules. Mol Pharm 2016;89:233–42.
27. Buchwald P, Bodor N. Quantitative structure-metabolism relationships: steric and nonsteric effects in the enzymatic hydrolysis of noncongener carboxylic esters. J Med Chem 1999;42:5160–8.
28. Chien DS, Sasaki H, Bundgaard H, Buur A, Lee VH. Role of enzymatic lability in the corneal and conjunctival penetration of timolol ester prodrugs in the pigmented rabbit. Pharm Res 1991;8:728–33.
29. Huang HP, Ayres JW. Dyphylline prodrugs: plasma hydrolysis and dyphylline release in rabbits. J Pharm Sci 1988;77:104–9.
30. Burke PJ, Hamilton JZ, Pires TA, Setter JR, Hunter JH, Cochran JH, et al. Development of novel quaternary ammonium linkers for antibody-drug conjugates. Mol Cancer Ther 2016;15:938–45.
31. Burke PJ, Jeffrey SC, Hamilton JZ, inventors; Targeted delivery of tertiary amine-containing drug substances. International patent number WO 2016/040684 A1. March 17, 2016.
32. Jeffrey SC, Andreyka JB, Bernhardt SX, Kissler KM, Kline T, Lenox JS, et al. Development and properties of beta-glucuronide linkers for monoclonal antibody-drug conjugates. Bioconjug Chem 2006;17:831–40.
33. Lyon RP, Bovee TD, Doronina SO, Burke PJ, Hunter JH, Neff-LaFord HD, et al. Reducing hydrophobicity of homogeneous antibody-drug conjugates improves pharmacokinetics and therapeutic index. Nat Biotechnol 2015;33:733–5.
34. Lewis TS, Gordon KA, Li F, Weimann A, Bruders R, Miyamoto JB, et al. Characterization and circumvention of drug resistance mechanisms in SGN-35 resistant HL and ALCL clonal cell lines. AACR Annual Meeting 2014; April 5–9, 2014; San Diego, CA.
35. Levengood MR, Zhang X, Hunter JH, Emmerton KK, Miyamoto JB, Lewis TS, et al. Orthogonal cysteine protection enables homogeneous multi-drug antibody-drug conjugates. Angew Chem Int Ed Engl 2017;56:733–7.
36. Lyon RP, Setter JR, Bovee TD, Doronina SO, Hunter JH, Anderson ME, et al. Self-hydrolyzing maleimides improve the stability and pharmacological properties of antibody-drug conjugates. Nat Biotechnol 2014;32:1059–62.
37. Walker MA, Dubowchik GM, Hofstead SJ, Trail PA, Firestone RA. Synthesis of an immunoconjugate of camptothecin. Bioorg Med Chem Lett 2002;12:217–9.
38. Li F, Emmerton KK, Jonas M, Zhang X, Miyamoto JB, Setter JR, et al. Intracellular released payload influences potency and bystander-killing effects of antibody-drug conjugates in preclinical models. Cancer Res 2016;76:2710–9.
39. Beck A, Goetsch L, Dumontet C, Corvaia N. Strategies and challenges for the next generation of antibody-drug conjugates. Nat Rev Drug Disc 2017;16:315–37.
40. Yu SF, Zheng B, Go M, Lau J, Spencer S, Raab H, et al. A novel anti-CD22 anthracycline-based antibody-drug conjugate (ADC) that overcomes resistance to auristatin-based ADCs. Clin Cancer Res 2015;21:3298–306.
41. Chen R, Hou J, Newman E, Kim Y, Donohue C, Liu X, et al. CD30 downregulation, MMAE resistance, and MDR1 upregulation are all associated with resistance to brentuximab vedotin. Mol Cancer Ther 2015;14:1376–84.
42. Christiansen J, Rajasekaran AK. Biological impediments to monoclonal antibody-based cancer immunotherapy. Mol Cancer Ther 2004;3:1493–501.
43. Greiner JW. Modulation of antigen expression in human tumor cell populations. Cancer Invest 1986;4:239–56.
44. Szakacs G, Paterson JK, Ludwig JA, Booth-Genthe C, Gottesman MM. Targeting multidrug resistance in cancer. Nat Rev Drug Disc 2006;5:219–34.
45. Fecik RA, Peterson MT, inventors; Therapeutic compounds. International patent number WO 2015/057585 A1. April 23, 2015.
46. Cheng H, Cong Q, Gangwar S, inventors; Antiproliferative compounds, conjugates thereof, methods therefor, and uses thereof. US patent 8,394,922 B2. March 12, 2013.
47. Richter W, inventor; Cytotoxic tubulysin compounds for conjugation. International patent number WO 2015/113760 A1. August 6, 2015.
48. O'Brien C, Cavet G, Pandita A, Hu X, Haydu L, Mohan S, et al. Functional genomics identifies ABCC3 as a mediator of taxane resistance in HER2-amplified breast cancer. Cancer Res 2008;68:5380–9.